Numerical discovery and continuation of points of infinitesimal homeostasis

Graham M. Donovan

Department of Mathematics, University of Auckland, Auckland, 1142 New Zealand

ABSTRACT

Homeostasis is the biological notion of certain outputs being stable with respect to input perturbations, at least over a relatively broad range. In general this is a result of coordination of regulatory mechanisms, and is thought to occur throughout biology. Recently the mathematical concept of *infinitesimal homeostasis* has been introduced, with the key idea being that the emergence of homeostasis is governed by certain geometric structures; these have previously been found in several mathematical models of biological processes. The theory of infinitesimal homeostasis has been applied to several specific classes of problems. Here we propose a more general method which allows for discovery of points of infinitesimal homeostasis, as well as their continuation, without imposing strong conditions on the underlying systems. The central idea is to construct an augmented system in which the desired point(s) of infinitesimal homeostasis occur as equilibria of the augmented system. The proposed method is developed and tested on several examples, ranging from synthetic test problems to examples drawn from the literature.

1. Introduction

Homeostasis is a biological concept in which regulatory mechanisms coordinate in order to ensure that certain system outputs are insensitive to input perturbations over a relatively broad range. A classic example is mammalian body temperature (thermoregulation) in which core body temperature is close to constant over a relatively broad range of ambient temperatures [1]. Many other biological processes are thought to be homeostatic, and the literature abounds with examples, ranging from insulin [2] and cholestorol regulation [3] to lymphocyte counts [4] and many more.

More recently the concept of *infinitesimal homeostasis* has been introduced, which formalizes the mathematical structures by which homeostasis might be expected to occur [5–7]. The central idea is that certain geometric structures govern the occurrence of homeostatic regions, and that these can be described in terms of appropriate local conditions on the derivatives of the equilibria with respect to the parameters. An outline of this theory is presented in Section 2 to give appropriate context.

This manuscript is concerned principally with the problem of discovery; that is, locating points of infinitesimal homeostasis. Previous work has shown methods which are applicable under certain (relatively strong) assumptions, but here we aim for a more general approach. While the principal concern is discovery, it is also worthwhile considering the potential for continuation; that is, once a point of infinitesimal homeostasis has been discovered, can its progression and

change through parameter space be tracked? If so, the discovery process can then be easily extended to a more complete understanding of the infinitesimal homeostasis points of a given system.

We propose a method based on continuous gradient descent in an augmented system which allows both discovery and continuation of points of infinitesimal homeostasis. The central idea is that points of infinitesimal homeostasis will be attracting equilibria in the (newly constructed) augmented system. The difficulty of the discovery process will then depend upon the basins of attraction of those equilibria. Once such a point has been located, standard continuation methods can then be used to continue the equilibria of the augmented system [8]. We develop this method and demonstrate its utility in a series of examples ranging from synthetic test problems to gene regulatory networks. Throughout this we concern ourselves principally with one particular type of infinitesimal homeostasis. Extension of this approach to other types is discussed but not explicitly undertaken.

2. Infinitesimal homeostasis

The concept of infinitesimal homeostasis has been developed in a recent series of papers [5–7,9]. Here we present a brief outline which allows the method proposed here to be understood in isolation, but this is by no means a complete presentation and the reader is referred to those works for most details. We begin by considering a system of first-order ordinary differential equations, which might be thought to describe a mathematical model of a biological process:

E-mail address: g.donovan@auckland.ac.nz.

$$\dot{x} = f(x; p_1, p_2) \tag{1}$$

Here $x \in \mathbb{R}^n$ are the system variables, and we explicitly include the dependence upon two parameters p_1 and p_2 ($\in \mathbb{R}$). At equilibrium we have

$$f(x^*; p_1, p_2) = 0 \tag{2}$$

where the equilibrium x^* depends on the two parameters and so we write

$$x^* = \mathcal{X}(p_1, p_2). \tag{3}$$

It is important to note that in general we cannot assume an explicit form for the equilibrium. Now we look at nth component[1] of x and define $X = \mathcal{X}_n$. This ($X(p_1)$) is known as the input-output map. Points of infinitesimal homeostasis then satisfy conditions on the derivatives of X with respect to p_1 and/or p_2 (and in higher dimensional settings, more parameters still). One particular form of infinitesimal homeostasis, known as a chair, is defined by p_1 and p_2 such that

$$\frac{\partial X}{\partial p_1} = 0, \tag{4}$$

$$\frac{\partial^2 X}{\partial p_1^2} = 0, \tag{5}$$

$$\frac{\partial^3 X}{\partial p_1^3} \neq 0, \text{ and} \tag{6}$$

$$\frac{\partial^2 X}{\partial p_1 \partial p_2} \neq 0. \tag{7}$$

Such a point has the universal unfolding (describing changes under perturbation and up to changes in coordinates) given by $X(p_1, p_2) = \pm p_1^3 + p_1 p_2$. This is illustrated in Fig. 1, along with the unfolding perturbations (in $\pm p_2$) giving rise to monotonic behaviour and local extrema. The chair is thought to be an important form of infinitesimal homeostasis because it is robust and relatively common in biological models [6], and it is this form on which we focus for the remainder of this paper; however, other forms infinitesimal homeostasis also exist [6,7].

3. Gradient flow augmentation

We now describe the proposed method for efficiently locating points of infinitesimal homeostasis. The central idea is to define an appropriate potential $\mathcal{P}$ such that the augmented system

$$\dot{x} = f(x; p_1, p_2) \tag{8}$$

$$\dot{p} = -\nabla \mathcal{P}, \tag{9}$$

which contains both the original system dynamics (Eq. (1)) as well as gradient flow toward minima of the potential, has stable, attracting equilibria at (X, p_1, p_2) satisfying the chair conditions (Eqs. (4)–(7)). Here $p = [p_1, p_2]^\top$. Such a system could then be used for either chair finding, or continuation.

To do so we define

$$\mathcal{P} = \alpha \left(\frac{\partial X}{\partial p_1} \right)^2 + \beta \left(\frac{\partial^2 X}{\partial p_1^2} \right)^2 + \delta \Lambda \left(\frac{\partial^3 X}{\partial p_1^3} \right) + \gamma \Lambda \left(\frac{\partial^2 X}{\partial p_1 \partial p_2} \right) \tag{10}$$

with $\Lambda(\cdot)$ an appropriate function where $\Lambda(x) \sim 0$ for $x \neq 0$ and $\Lambda(x) \sim O(1)$ for $x \approx 0$. The weight parameters α, β, δ and γ (all ≥ 0) may be useful numerically but can otherwise be thought of as being equal to unity. In general it is not possible to construct this potential
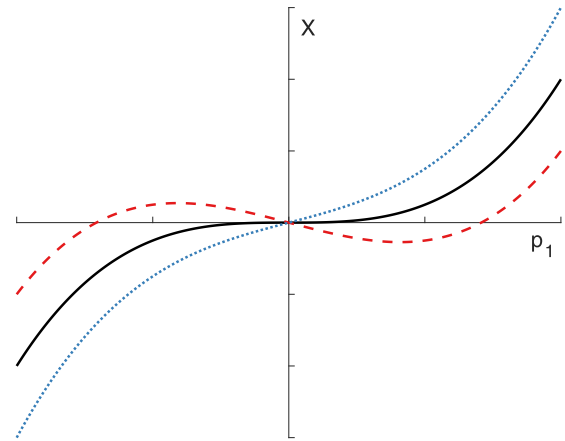

Fig. 1. Illustration of the chair form of infinitesimal homeostasis (black), along with unfolding curves showing monotonic behaviour (blue, dotted) and local extrema (red, dashed).

explicitly without an explicit form for X, which we cannot assume (though we will later consider a synthetic test problem in which this is possible).

However, $\mathcal{P}$ can still be approximated. One approach is to define an augmented system which allows approximation of $\nabla \mathcal{P}$. The idea is as follows. Suppose we wish to approximate $\frac{\partial X}{\partial p_1}$. To do so we can define a new variable x^+ where

$$\dot{x}^+ = f(x^+; p_1 + h, p_2), \tag{11}$$

that is, following the same dynamics as x but shifted in p_1-space. We then take

$$\frac{\partial X}{\partial p_1} \approx \frac{x^+ - x}{h} \tag{12}$$

which has error $O(h)$ as $t \to \infty$ for h small and $\lim_{t \to \infty} x = X$.

The same idea can be extended to the higher order derivatives involved in $\nabla \mathcal{P}$. However, rather than explicitly constructing the finite differences as done in the motivation above, in order to approximate $\nabla \mathcal{P}$ we instead define an appropriate higher order stencil which allows approximations of the derivatives involved via an appropriate interpolating polynomial on that stencil. Expanding $\nabla \mathcal{P}$ we have[2]

$$\nabla \mathcal{P} = \begin{pmatrix} 2\alpha \frac{\partial X}{\partial p_1} \frac{\partial^2 X}{\partial p_1^2} + 2\beta \frac{\partial^2 X}{\partial p_1^2} \frac{\partial^3 X}{\partial p_1^3} + \delta \Lambda' \left(\frac{\partial^3 X}{\partial p_1^3} \right) \frac{\partial^4 X}{\partial p_1^4} + \gamma \Lambda' \left(\frac{\partial^2 X}{\partial p_1 \partial p_2} \right) \frac{\partial^3 X}{\partial p_1^2 \partial p_2} \\ 2\alpha \frac{\partial X}{\partial p_1} \frac{\partial^2 X}{\partial p_1 \partial p_2} + 2\beta \frac{\partial^2 X}{\partial p_1^2} \frac{\partial^3 X}{\partial p_1^2 \partial p_2} + \delta \Lambda' \left(\frac{\partial^3 X}{\partial p_1^3} \right) \frac{\partial^4 X}{\partial p_1^3 \partial p_2} + \gamma \Lambda' \left(\frac{\partial^2 X}{\partial p_1 \partial p_2} \right) \frac{\partial^3 X}{\partial p_1 \partial p_2^2} \end{pmatrix}. \tag{13}$$

We define our stencil on the following points: $x_{-2,-2}, x_{-2,0}, x_{-1,-1}, x_{-1,2}, x_{0,0}, x_{1,-2}, x_{1,1}, x_{2,-1}, x_{2,2}$, where the subscripts indicate shifts of h with respect to p_1 and p_2 respectively[3] – see also Fig. 2 for a schematic illustration. By extension we have at each stencil point the shifted dynamics

$$\dot{x}_{i,j} = f(x_{i,j}; p_1 + ih, p_2 + jh). \tag{14}$$

Now we define a polynomial

$$C := c_1 + c_2 p_1 + c_3 p_2 + c_4 p_1 p_2 + c_5 p_1^2 + c_6 p_1^3 + c_7 p_1^2 p_2 + c_8 p_1 p_2^2 + c_9 p_1^4 \tag{15}$$

---

[1] More general reductions ($\mathbb{R}^n \to \mathbb{R}$) can be used, but here we consider taking a single component for simplicity.

[2] In the following we neglect the $\frac{\partial^4 X}{\partial p_1^2 \partial p_2}$ term, but this can be incorporated in the same way.

[3] We use the same h for steps in both p_1 and p_2 for clarity, though this can easily be generalized either through explicit use of h_1 and h_2, or by appropriate rescaling of p_1 and p_2.
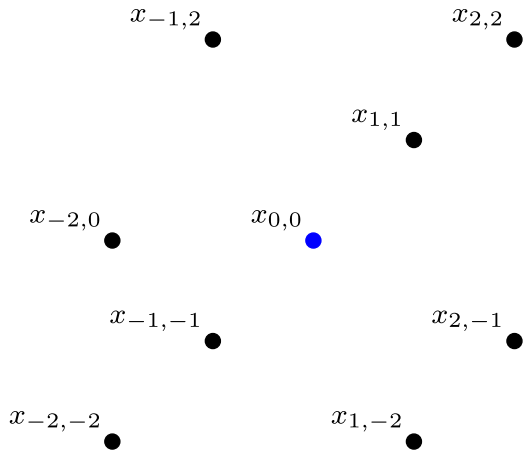
Fig. 2. Stencil in (p_1, p_2) space.

with terms chosen to represent appropriate derivatives. The coefficients c_1 through c_9 can be determined by interpolation on the 9-point stencil by solution of the linear system.[4]

We then compute derivatives of Eq. (15) as needed to complete Eq. (13) – that is, $\frac{\partial C}{\partial p_1}$, $\cdots$, $\frac{\partial^3 C}{\partial p_1 \partial p_2^2}$, $\frac{\partial^4 C}{\partial p_1^4}$. By substituting into Eq. (13) we obtain $\nabla\mathcal{P}$ in terms of $c_1 - c_9$ and hence in terms of x at the stencil points (via solution of the linear system). Explicitly this yields

$$\nabla\mathcal{P} \approx \begin{pmatrix} 4\alpha c_2 c_5 + 24\beta c_5 c_6 + 24\delta c_9 \mathcal{N}(6c_6) + 2\gamma c_7 \mathcal{N}(c_4) \\ 2\alpha c_2 c_4 + 8\beta c_5 c_7 + 2\gamma c_8 \mathcal{N}(c_4) \end{pmatrix}. \tag{16}$$

In principle this can be expressed explicitly in terms of the values at the stencil points, but this involves the solution of the 9x9 linear system; in practice it is easier to leave it in this form and solve the linear system directly. Using the ordering of the stencil points given above, the Vandermonde coefficient matrix is given by

$$A = \begin{bmatrix} 1 & -2h & -2h & 4h^2 & 4h^2 & -8h^3 & -8h^3 & -8h^3 & 16h^4 \\ 1 & -2h & 0 & 0 & 4h^2 & -8h^3 & 0 & 0 & 16h^4 \\ 1 & -h & -h & h^2 & h^2 & -h^3 & -h^3 & -h^3 & h^4 \\ 1 & -h & 2h & -2h^2 & h^2 & -h^3 & 2h^3 & -4h^3 & h^4 \\ 1 & 0 & 0 & 0 & 0 & 0 & 0 & 0 & 0 \\ 1 & h & -2h & -2h^2 & h^2 & h^3 & -2h^3 & 4h^3 & h^4 \\ 1 & h & h & h^2 & h^2 & h^3 & h^3 & h^3 & h^4 \\ 1 & 2h & -h & -2h^2 & 4h^2 & 8h^3 & -4h^3 & 2h^3 & 16h^4 \\ 1 & 2h & 2h & 4h^2 & 4h^2 & 8h^3 & 8h^3 & 8h^3 & 16h^4 \end{bmatrix}$$

where

$$A[c_1, c_2, ...c_9]^\top = [x_{-2,-2}, x_{-2,0}, x_{-1,-1}, x_{-1,2}, x_{0,0}, x_{1,-2}, x_{1,1}, x_{2,-1}, x_{2,2}]^\top. \tag{17}$$

Eqs. (8) and (9) can then be combined with (16) to form the augmented system.

In the examples that follow, this augmented system is solved using a variable step-size 4th-order Runge-Kutta method. Initial conditions for the augmented system are obtained by first running the intrinsic dynamics so as to start sufficiently near the equilibrium manifold.

4. Results

We now demonstrate the application of this method to several test problems.

---

[4] The design of the above stencil may have previously seemed arbitrary; in fact, it is carefully chosen so that the linear system is full rank [10,11].

4.1. GRN model

First we consider the gene regulatory network (GRN) model of [5]. This model has been shown to have a known chair point. This is a feed-forward network, with structure illustrated in Fig. 3. Briefly, x, y and z indicate three species, with the r subscript being mRNA concentration and the p subscript being protein concentration. The interested reader is referred to Antoneli et al. [5] for full details. The model equations are given by

$$\begin{aligned} \dot{x}_r &= -\delta_x x_r + \mathcal{S}(x_p) + I \\ \dot{x}_p &= -\alpha_x x_p + x_r \\ \dot{y}_r &= -\delta_y y_r + \mathcal{S}(x_p) \\ \dot{y}_p &= -\alpha_y y_p + y_r \\ \dot{z}_r &= -\delta_z z_r + \mathcal{S}(x_p + y_p) \\ \dot{z}_p &= -\alpha_z z_p + z_r \end{aligned}$$

with $\mathcal{S}(x) = \frac{1}{1+x^2}$.

Using the method proposed in Section 3 we construct the augmented system and potential $\mathcal{P}$ and simulate the dynamics of this system, shown in Fig. 4. The upper panel shows trajectories from random initial conditions in (p_1, p_2) space with steady state locations shown as red x's. The equilibrium surface is shown explicitly for visualization, though in general this would not be a practical element of the discovery calculation. The lower panels illustrate the proposed chair point and its unfolding in p_2, where the central point is found by taking the median across all simulated trajectories. In short, the gradient flow augmented system does indeed have an attracting equilibrium at the chair point, and it has a sufficiently large basin of attraction that it can be located using randomized initial conditions.

4.2. Generalized GRN model

The GRN model of Section 4.1 can be generalized into a double feed-forward network. The extended network is illustrated schematically in Fig. 5 and the model equations are given by

$$\begin{aligned} \dot{x}_r &= -\delta_x x_r + \mathcal{S}(x_p) + I_1 \\ \dot{x}_p &= -\alpha_x x_p + x_r \\ \dot{u}_r &= -\delta_u u_r + \mathcal{S}(u_p) + I_2 \\ \dot{u}_p &= -\alpha_u u_p + u_r \\ \dot{y}_r &= -\delta_y y_r + \mathcal{S}(x_p + u_p) \\ \dot{y}_p &= -\alpha_y y_p + y_r \\ \dot{z}_r &= -\delta_z z_r + \mathcal{S}(x_p + y_p + u_p) \\ \dot{z}_p &= -\alpha_z z_p + z_r. \end{aligned}$$

While this model shares obvious commonalities with that of the previous section, it has not previously been shown to have a chair point of infinitesimal homeostasis. Again applying the gradient flow augmentation method we obtain trajectories and proposed chair point and unfolding as shown in Fig. 6. Again this method has generated an attracting equilibrium at the chair point, with sufficient basin of attraction.

4.3. Synthetic test problem

We also demonstrate the method with a synthetic problem which

1. Contains a known chair (by construction), and
2. Allows explicit construction of $\nabla\mathcal{P}$.

This allows comparison of the $\nabla\mathcal{P}$ approximation method with an explicit version. Thus we take

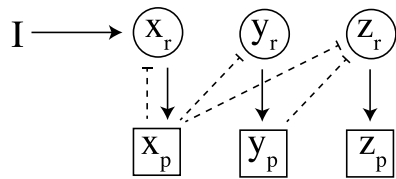$$\dot{x} = X(p_1, p_2) - x \tag{18}$$

Fig. 3. Schematic illustration of the GRN model. Solid arrows indicate positive coupling and dashed indicate coupling which may be either positive or negative [5].

where

$$X(p_1, p_2) = p_1^3 - p_1 p_2. \tag{19}$$

Then

$$\mathcal{P} = \alpha(3p_1^2 + p_2)^2 + \beta(6p_1)^2 \tag{20}$$

and, noting that both $\Lambda(\cdot)$ terms are identically zero for this problem, we have

$$\nabla \mathcal{P} = \begin{pmatrix} 36\alpha p_1^3 + 12\alpha p_1 p_2 + 72\beta p_1 \\ 6\alpha p_1^2 + 2\alpha p_2 \end{pmatrix}. \tag{21}$$

The Jacobian can of course be computed as well,

$$\mathcal{J}|_{(0,0,0)} = \begin{bmatrix} -1 & 0 & 0 \\ 0 & -72\beta & 0 \\ 0 & 0 & -2\alpha \end{bmatrix}, \tag{22}$$

suggesting taking $\beta = 1/72$ and $\alpha = 1/2$. A numerical demonstration of the attracting gradient flow dynamics is shown in Fig. 7, with the explicit potential version shown in the left panel and the approximated potential version shown in the right panel. From this we observe that both cases share the same basic structure on the equilibrium manifold, but that the off-manifold dynamics are altered by the approximation of ∇P, as is expected given the nature of that approximation.

5. Discussion and conclusions

Infinitesimal homeostasis is a mathematical extension of the biological notion of homeostasis, and is thought to occur in many systems [12,13]. Previous work has considered many important theoretical issues, particularly in specific classes of systems, and here we explore a proposed method for locating points of infinitesimal homeostasis in more general systems. The proposed method is based on gradient flow in an augmented system with the central notion that the derived system will have equilibria at points of infinitesimal homeostasis (in the original system). If these points are attracting and have sufficient basins of attraction, this can be used for discovery of points of infinitesimal homeostasis. Furthermore any equilibria in the augmented system can also be used in standard numerical continuation of equilibria – that is, understanding how the equilibria change as the
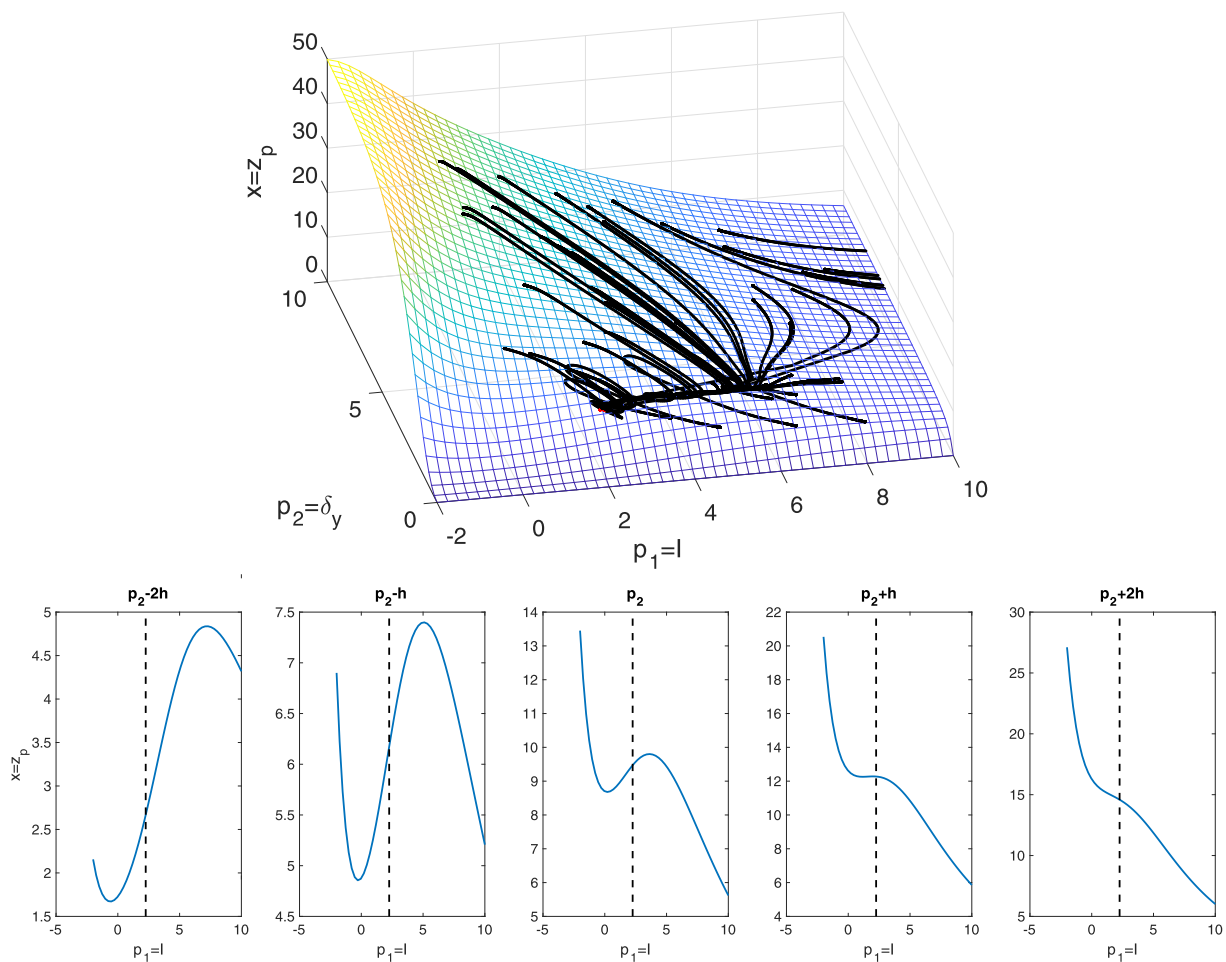

Fig. 4. Upper: Equilibrium surface and sample of attracting gradient flow dynamics in GRN system with approximated potential. Initial conditions are selected randomly, and final (steady state) is indicated by a red *x*. Here we seek a chair in $(z_p; I, \delta_y)$, with fixed parameters $\delta_x = 10$, $\delta_z = 0.1$, $\alpha_x = 0.4$, $\alpha_y = 0.3$, and $\alpha_z = 0.2$. Here $\Lambda(x) = \text{sech}(x)$. Lower: unfolding about the located point.
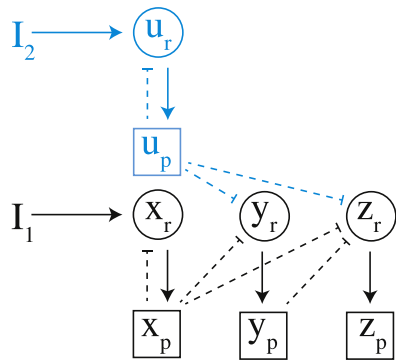
Fig. 5. Schematic illustration of the double feed-forward GRN model. For convenience the changes from Fig. 3 are indicated in blue. Solid arrows indicate positive coupling and dashed indicate coupling which may be either positive or negative.

parameters are varied – and thus by extension to explore the progression of points of infinitesimal homeostasis throughout parameter space. We have demonstrated the application of this method in several different problems, ranging from synthetic test problems through to examples drawn from the literature. It is also worth emphasizing that while several of the test problems are feed-forward networks (i.e. of a specific class of problem which admits more detailed analysis), this is not a requirement of this method.

The central idea of this method is attempting to exploit the simultaneous evolution of both the underlying system and the gradient flow in parameter space in order to locate points of infinitesimal homeostasis more efficiently. By way of comparison, an alternate approach might seek to construct the input-output map (or equilibrium manifold) directly before then seeking points of infinitesimal homeostasis within that. The potential advantages of the simultaneous approach is that it eliminates the need for many evaluations of the input-output map, and also that this construction is naturally suited to continuation (once a point of infinitesimal homeostasis is found). The potential disadvantages are that the augmented system has effective dimension $MN + 2$ where N is the original system size and M is the stencil size, and also that the potential flow dynamics may be inaccurate if the errors in approximating the local derivatives (e.g. Eq. (12)) are large, either because t is insufficiently large or because the initial conditions are not in the basin of attraction of X. That said, these problems are largely confined to application of this method to discovery and not to continuation, because in the latter case it should almost always be possible to start sufficiently close to the point of infinitesimal homeostasis.

We have derived and demonstrated a method for locating chair points in a 2D parameter space (e.g. (p_1, p_2) space) but the ideas could be modified to other related settings. One alternative approach would be to construct the augmented system in p_1 only and neglect the mixed partial term (e.g. $p = p_1$ and $\gamma = 0$). The required stencil then consists only of 5 points. It may be necessary to perform root-finding in p_2 in order to find a chair point, but this reduced formulation may be
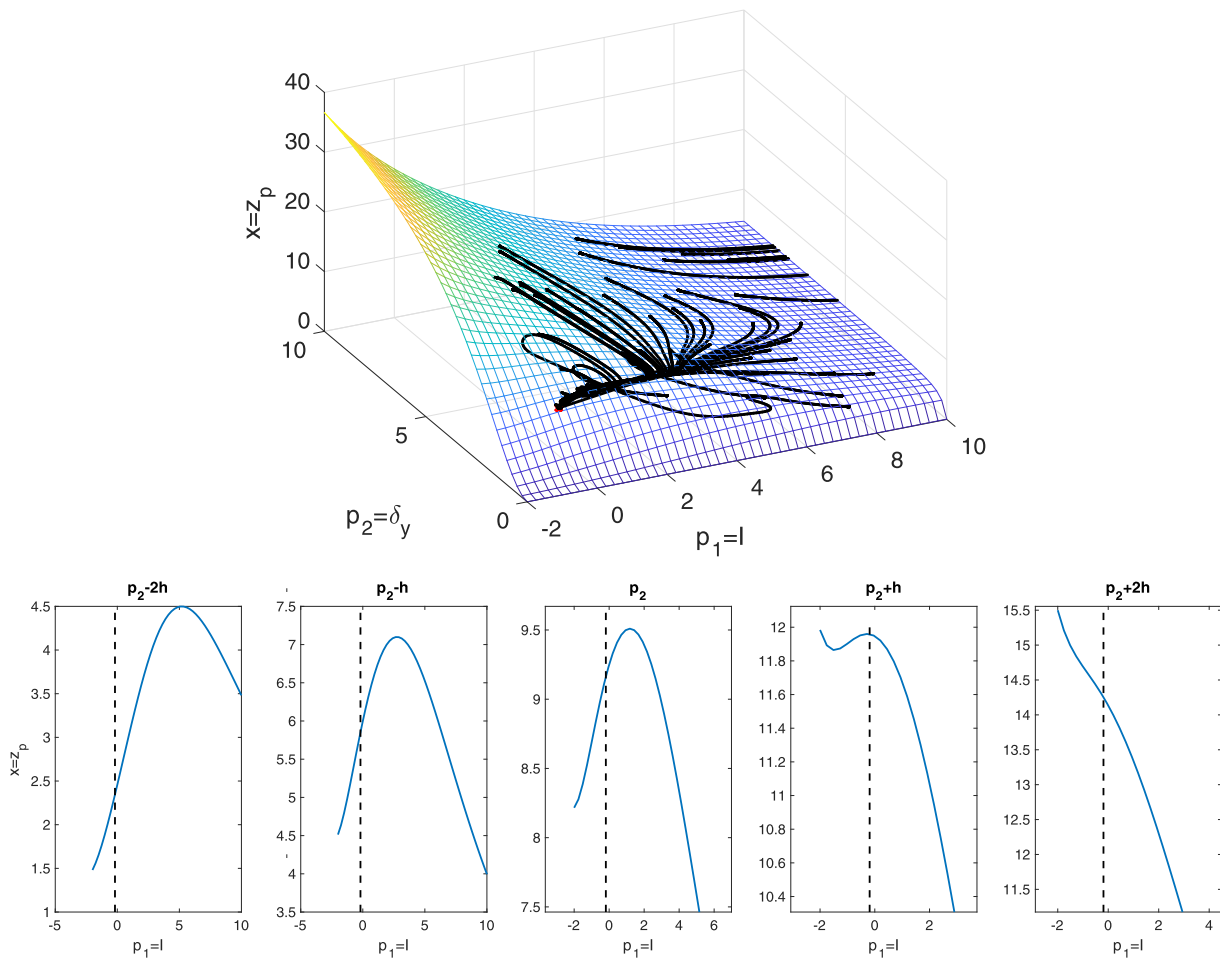

Fig. 6. Upper: Equilibrium surface and sample of attracting gradient flow dynamics in generalized GRN system with estimated potential. Here we seek a chair in (z_p; I, δ_y), with fixed parameters $\delta_x = 10$, $\delta_u = 10$, $\delta_z = 0.1$, $\alpha_x = 0.4$, $\alpha_u = 0.4$, $\alpha_y = 0.3$, $\alpha_z = 0.2$ and $I_2 = 1.5$. Here $\Lambda(x) = \mathrm{sech}(x)$. Lower: unfolding about the located point.
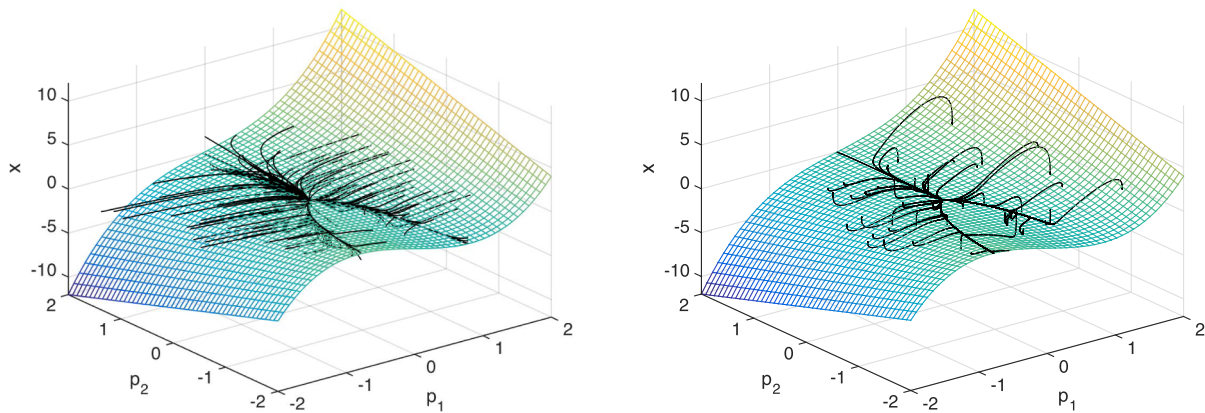
Fig. 7. Equilibrium surface and sample of attracting gradient flow dynamics in the synthetic system with: explicit potential (left panel) and approximated potential (right panel).

sufficient for continuation.

Similarly these ideas might be extended to higher-dimensional versions of infinitesimal homeostasis. For example, the *hyperbolic umbilic* is codimension 3 and has universal unfolding $p_1^3 + p_2^3 + ap_1p_2 + bp_1 + cp_2$. A minimal version of gradient flow augmentation for the hyperbolic umbilic would involve a 15-point stencil (e.g. akin to the 5-point stencil in 1D for the chair). This might be practical, given the computations done here with a 9-point stencil. A full 5D stencil which explicitly captures the unfolding of the hyperbolic umbilic could theoretically be constructed in the same way, but the augmented system would probably be too large to be of practical use in most situations.

In the development of this method we have worked directly with derivatives of the input-output map ($X(p_1, p_2)$) before approximating these. An alternate approach, proposed by Golubitsky and Stewart [6], is to instead differentiate Eq. (2) implicitly and thus to work instead with derivatives of f. It remains to be seen if this formulation is better able to capture the desired dynamics.

More speculatively, there is also a potential connection with fast-slow systems [14] which may be of interest, in terms of the potential separation of timescales between the intrinsic system dynamics and the potential flow dynamics. That is, the potential flow might be though of as occurring on the equilibrium manifold (i.e. the input-output map). Thus, depending on these timescales, methods from fast-slow systems might be deployed in further understanding of the underlying behaviour of this method. However it is yet unclear how these might be treated in the general case; in the synthetic test problem we explicitly balanced the eigenvalues through our choice of α and β, but it is unclear how this might be done without such an explicit formulation.

Taken together, these results suggest that the proposed approach –

gradient flow in an augmented system – is a plausible method for numerically locating and continuing points of infinitesimal homeostasis without strong restrictions on the underlying system.

References

[1] H.B. Theodor, Heat regulation: homeostasis of central temperature in man, Physiol. Rev. 49 (4) (1969) 671–759.

[2] D.R. Matthews, J.P. Hosker, A.S. Rudenski, B.A. Naylor, D.F. Treacher, R.C. Turner, Homeostasis model assessment: insulin resistance and β-cell function from fasting plasma glucose and insulin concentrations in man, Diabetologia 28 (7) (1985) 412–419.

[3] M.S. Brown, J.L. Goldstein, et al., A receptor-mediated pathway for cholesterol homeostasis, Science 232 (4746) (1986) 34–47.

[4] E.C. Butcher, L.J. Picker, Lymphocyte homing and homeostasis, Science 272 (5258) (1996) 60–67.

[5] F. Antoneli, M. Golubitsky, I. Stewart, Homeostasis in a feed forward loop gene regulatory motif, J. Theor. Biol. 445 (2018) 103–109.

[6] M. Golubitsky, I. Stewart, Homeostasis, singularities, and networks, J. Math. Biol. 74 (1–2) (2017) 387–407.

[7] M. Golubitsky, I. Stewart, Homeostasis with multiple inputs, SIAM J. Appl. Dyn. Syst. 17 (2) (2018) 1816–1832.

[8] E.L. Allgower, G. Kurt, Numerical Continuation Methods: An Introduction, vol. 13, Springer Science & Business Media, 2012.

[9] M. Reed, J. Best, M. Golubitsky, I. Stewart, H.F. Nijhout, Analysis of homeostatic mechanisms in biochemical networks, Bull. Math. Biol. 79 (11) (2017) 2534–2557.

[10] R.B. Guenther, E.L. Roetman., Some observations on interpolation in higher dimensions, Math. Comput. 24 (111) (1970) 517–522.

[11] M. Gasca, T. Sauer, Polynomial interpolation in several variables, Adv. Comput. Math. 12 (4) (2000) 377.

[12] W. Duncan, J. Best, M. Golubitsky, H.F. Nijhout, M. Reed, Homeostasis despite instability, Math. Biosci. 300 (2018) 130–137.

[13] G.M. Donovan, Biological version of Braess' paradox arising from perturbed homeostasis, Phys. Rev. E 98 (6) (2018) 062406.

[14] T. Witelski, M. Bowen, Fast/slow dynamical systems, Methods of Mathematical Modelling, Springer, 2015, pp. 201–213.